Adsorption of pharmaceuticals from biologically treated municipal wastewater using paper mill sludge-based activated carbon

Carla Patrícia Silva[a*], *Guilaine Jaria*[a], *Marta Otero*[b], *Valdemar I. Esteves*[a], *Vânia Calisto*[a]

[a]Department of Chemistry and CESAM (Centre for Environmental and Marine Studies), University of Aveiro, Campus de Santiago, 3810-193 Aveiro, Portugal

[b]Department of Environment and Planning and CESAM (Centre for Environmental and Marine Studies), University of Aveiro, Campus de Santiago, 3810-193 Aveiro, Portugal

Declarations of interest: none

[*]Corresponding author:
Postal Address: Department of Chemistry and CESAM (Centre for Environmental and Marine Studies), University of Aveiro, Campus de Santiago, 3810-193 Aveiro, Portugal
Phone: +351 234 370360; Fax: +351 234 370084
E-mail address: patricia.silva@ua.pt

ABSTRACT

A waste-based alternative activated carbon (AAC) was produced from paper mill sludge under optimized conditions. Aiming its application in tertiary wastewater treatment, AAC was used for the removal of carbamazepine, sulfamethoxazole and paroxetine from biologically treated municipal wastewater. Kinetic and equilibrium adsorption experiments were run under batch operation conditions. For comparison purposes, they were also performed in ultrapure water and using a high-performance commercial AC (CAC). Adsorption kinetics was fast for the three pharmaceuticals and similar onto AAC and CAC in either wastewater or ultrapure water. However, matrix effects were observed in the equilibrium results, being more remarkable for AAC. These effects were evidenced by Langmuir maximum adsorption capacities (q_m, mg g^{-1}): for AAC, the lowest and highest q_m were 194 ± 10 (SMX) and 287 ± 9 (PAR), in ultrapure water, and 47 ± 1 (SMX) and 407 ± 14 (PAR), in wastewater; while for CAC, the lowest and highest q_m were 118 ± 7 (SMX) and 190 ± 16 (PAR) in ultrapure water, and 123 ± 5 (SMX) and 160 ± 7 (CBZ) in wastewater. It was found that the matrix pH played a key role in these differences by controlling the surface electrostatic interactions between pharmaceutical and AC. Overall, it was evidenced the need of adsorption results in real matrices and demonstrated that AAC is a promising option to be implemented in tertiary wastewater treatments for pharmaceuticals' removal.

KEYWORDS: Waste-based carbons; Waste valorization; Emerging pollutants; Adsorption; Water quality

1. INTRODUCTION

In the European Union, from the 2.3 billion tonnes of waste that are produced annually, 10% include municipal waste and 90% industrial, agricultural and commercial-related wastes (Grace et al., 2016). In constrast to the current take-make-dispose industrial model, a circular economy is a regenerative model under which wastes are either turned into new products or used as new resources for other products. On the other hand, concern about the presence of emerging contaminants such as pharmaceuticals in water resources has been growing over the last years. Due to their continuous input and persistence, these compounds pose a long-term risk to the aquatic organisms, namely in what respects to endocrine disruption or antimicrobial resistance (Silva et al., 2017). It is well known that effluents from sewage treatment plants (STPs) are the main source of these pollutants in the aquatic environment. For this reason, a great research effort has been carried out on alternative or additional treatments to those usually applied in STPs. Among them, adsorptive processes have been amongst most recommended due to their efficiency, versatility, simplicity and the non-formation of hazardous products (Silva et al., 2017). Furthermore, the incorporation of adsorption processes as tertiary treatments into current STPs is quite feasible, which is essential from a practical point of view (Coimbra et al., 2015).

In the described context, the utilization of waste-based adsorbents has emerged as a sustainable alternative to conventional activated carbons (AC) from non-renewable precursors. Different wastes have been used as raw materials and subjected to diverse procedures aiming the production of alternative adsorbents for the removal of pharmaceuticals from water (e.g. Mestre et al., 2009, 2011, 2014, 2017). Paper mill sludge is generated in huge amounts from wastewater treatment at the paper industry (each ton of paper means an average production of 40-50 kg of sludge) and its use as

raw material in the preparation of adsorbents for the adsorption of pharmaceuticals was firstly reported by Calisto et al. (2014). In that work, different biochars were obtained through the pyrolysis of primary and biological paper mill sludge under different conditions, which were characterized and used for the adsorption of citalopram from water. Results shown that paper mill sludge was a promising raw material for the aforementioned application, which besides means the valorization of such waste (Calisto et al., 2014). The promising results obtained for the paper mill sludge based biochars encouraged the study of the production of an AC from the referred waste. A full factorial design was carried out to determine the most favourable route to produce a powdered alternative activated carbon (AAC) with improved and promising properties (a high specific surface area (S_{BET}) of 1627 m^2 g^{-1} and very good responses in terms of adsorption percentage for pharmaceuticals of different classes). However, as most of the published literature on the utilization of alternative adsorbents, the referred results on the utilization of paper mill sludge-based adsorbents were obtained in ultrapure water. Therefore, in view of the practical application of the produced materials in real systems, the evaluation of the performance of the optimized AAC in wastewater was explicitely outlined as future work by Jaria et al. (2018). Simultaneously, stricter legislation on the discharge of pharmaceuticals into the environment is expected in the near future, and therefore, STPs will need to upgrade the wastewater treatments to cope with new regulations. Consequently, the present work aimed at assessing the practical utilization of the previously optimized powdered AAC in the tertiary treatment of wastewater for the removal of pharmaceuticals frequently found in aquatic environments, from different pharmacological classes and with distinct physico-chemical properties. Also, the performance of a commercial activated carbon (CAC) was evaluated under the same conditions for comparison. For these purposes, the adsorption kinetics, equilibrium

isotherms and adsorption capacity of AAC and CAC towards carbamazepine (CBZ), sulfamethoxazole (SMX) and paroxetine (PAR) from biologically treated wastewater were determined.

2. EXPERIMENTAL

2.1 Reagents and materials

Pharmaceuticals used for the adsorption experiments were CBZ (Sigma Aldrich, 99%), SMX (TCI, >98%) and PAR (paroxetine-hydrochloride; TCI, >98%). All the pharmaceuticals solutions were prepared in ultrapure water (obtained from a Milli-Q Millipore system Milli-Q plus 185) or in wastewater collected from the effluent of a STP. In the production of AAC, the chemical activation process was performed using potassium hydroxide (KOH) (EKA PELLETS, ≥86%), while HCl (AnalaR NORMAPUR, 37%) was used for the washing step.

The CAC used in this work for comparison purposes was a high performance commercial AC from Norit (SAE SUPER 8003.6), kindly supplied by Salmon & CIA.

2.2 Preparation of the alternative activated carbon (AAC)

The AAC was here produced accordingly to the optimal conditions previously determined through a full factorial design and described in detail by Jaria et al. (2018). To sum up, after collection of primary sludge (PS) from a paper industry, PS was dried at room temperature followed by a 24 h period at 105 ºC in an oven and then it was grinded with a blade mill. The grinded PS was impregnated with KOH (activating agent) in a 1:1 activating agent/PS ratio and the mixture was stirred in an ultrasonic bath during 1 h and then left to dry at room temperature. Dried material was subjected to pyrolysis in a muffle (Nüve, series MF 106, Turkey) at 800ºC under controlled N_2 atmosphere during 150 min. The resulting material was washed with 1.2 M HCl in order

to remove ashes and other inorganic material and afterwards washed with distilled water until reaching a neutral pH. Finally, the produced AAC was dried in an oven for 24 h at 105 ºC.

2.3 Characterization of activated carbons

The characterization of AAC in terms of nitrogen adsorption isotherms for the determination of S_{BET} and microporosity, total organic carbon (TOC), point of zero charge (pH_{pzc}), the main surface acidic and basic functional groups (Boehm's titration), proximate and ultimate analysis and scanning electron microscopy (SEM) analysis was described in detail by Jaria et al. (2018). In this work, the same procedures were used for the characterization of the CAC and in order to determine its S_{BET} and microporosity, TOC and IC, pH_{pzc}, proximate and ultimate analysis, and SEM. Briefly, for the determination of S_{BET} (calculated from the Brunauer-Emmett-Teller equation (Brunauer et al., 1938) in the relative pressure range 0.01–0.1) and micropore volume (W_0; determined applying the Dubinin-Astakhov equation (Dubinin, 1966) to the lower relative pressure zone of the nitrogen adsorption isotherm), isotherms were acquired at 77 K using a Micromeritics Instrument, Gemini VII 2380 after the outgassing of the materials overnight at 120 ºC. TC and IC analyses were performed always in triplicate using a TOC analyzer (Shimadzu, model TOC-V_{CPH}, SSM-5000A, Japan). TOC was calculated by difference between total carbon (TC) and total inorganic carbon (IC). The pH_{pzc} was determined by the pH drift method as described by Jaria et al. (2015). Proximate analysis was performed by thermogravimetric analysis (TGA) using a Setaram thermobalance, model Setsys Evolution 1750 (S type sensor). Standard methods were followed to determine the moisture (UNE 32002) (AENOR, 1995), volatile matter (UNE 32019) (AENOR, 1985) and ash content (UNE 32004) (AENOR,

1984). Ultimate analysis was performed in a LECO CHNS-932 analyser using standard methods to determine C, H, N and S as detailed in Calisto et al. (2014). SEM was used to assess the ACs' surface morphology through a Hitachi SU-70.

Moreover, for a deeper characterization of the produced AAC, this carbon was characterized by X-ray Photoelectron Spectroscopy (XPS) analysis, which was performed in an Ultra High Vacuum (UHV) system with a base pressure of 2×10^{-10} mbar and equipped with a hemispherical electron energy analyser (SPECS Phoibos 150), a delay-line detector and a monochromatic Al Kα (1486.74 eV) X-ray source. High resolution spectra were recorded at normal emission take-off angle and with a pass-energy of 20 eV, providing an overall instrumental peak broadening of 0.5 eV.

2.4 Biologically treated municipal wastewater

Wastewater for the adsorption experiments was collected at three collection campaings (between May and September 2017) from a local STP. This STP was designed to serve 159 700 population equivalents and receives an average daily flow of 39 278 m^3 day^{-1}. In the STP, wastewater is subjected to primary and then biological treatment.

Wastewater was collected after the biological decanter, which corresponds to the final treated effluent that is discharged into the environment (in this case, into the sea, at ~3 km from the coast). Immediately after collection, wastewater was filtered through 0.45 μm, 293 mm Supor® membrane disc filters (Gelman Sciences) and stored at 4 °C until use, which occurred within a maximum of 15 days.

Wastewater collected in each campaign was characterized by conductivity (WTW meter), pH (pH/mV/°C meter pHenomenal® pH 1100L, VWR) and TOC (Shimadzu, model TOC-V_{CPH}, SSM-5000A).

2.5 Adsorption experiments

Batch adsorption experiments were performed by contacting the adsorbents (AAC or CAC) with solutions of pharmaceutical (CBZ, SMX or PAR) prepared either in ultrapure or in the collected wastewater. Pharmaceutical solutions of CBZ, SMX or PAR, with an initial concentration (C_0) of 5 mg L^{-1} were shaken together with a known concentration (M) of the corresponding adsorbent in polypropylene tubes. The tubes were shaken in a head-over-head shaker (Heidolph, Reax 2) at 80 rpm, under controlled temperature (25.0 ± 0.1 ºC). After shaking, solutions were filtered through 0.2 µm PVDF filters (Whatman) and analysed for the residual concentration of pharmaceutical by micellar electrokinetic chromatography (MEKC) (as described in section 2.6). Control experiments, i.e. the pharmaceutical solution in absence of adsorbent, were run in parallel. All experiments were run in triplicate.

2.5.1 Adsorption kinetics

The time needed to attain the adsorption equilibrium was determined by shaking single pharmaceutical solutions (in ultrapure water or wastewater) with the corresponding adsorbent (AAC or CAC) for different time intervals (between 5 and 360 min). In ultrapure water, for both AAC and CAC, the adsorbent concentration (M, g L^{-1}) was 0.020 g L^{-1} for all the pharmaceuticals. Meanwhile, when using wastewater, M was 0.020 g L^{-1} for CBZ and PAR and 0.10 g L^{-1} for SMX. Then, the amount of pharmaceutical adsorbed by mass unit of adsorbent at each time (q_t , mg g^{-1}) was calculated as:

$$q_t = \frac{(C_0 - C_t)}{M} \quad \text{(Eq. 1)}$$

where C_t (g L^{-1}) is the residual pharmaceutical concentration after shaking during the corresponding time (t, min).

The obtained experimental data were fitted to the pseudo-first (Eq. 2 (Lagergren, 1898)) and pseudo-second order (Eq. 3 (Ho and Mckay, 1999)) kinetic models using GraphPad Prism, version 5:

$$q_t = q_e(1 - e^{-k_1 t}) \quad \text{(Eq. 2)}$$

$$q_t = \frac{q_e^2 k_2 t}{1 + q_e k_2 t} \quad \text{(Eq. 3)}$$

where, t (min) represents the adsorbent/solution contact time, q_e the amount of pharmaceutical adsorbed when the equilibrium is attained (mg g^{-1}), and k_1 (min^{-1}) and k_2 (g mg^{-1} min^{-1}) the pseudo-first and pseudo-second order rate constant, respectively.

2.5.2 Adsorption equilibrium

Equilibrium adsorption experiments were performed by shaking single pharmaceuticals' solutions (CBZ, SMX or PAR) in either ultrapure or wastewater with a known M (0.008-0.050 g L^{-1} CBZ, SMX and PAR, in ultrapure water; 0.008-0.050 g L^{-1} CBZ and PAR, in wastewater; 0.02-0.2 g L^{-1} SMX, in wastewater) of AAC or CAC during the time needed to attain the equilibrium, as determined in the previous section. Then, the amount of pharmaceutical adsorbed by mass unit of adsorbent at the equilibrium (q_e , mg g^{-1}) was calculated with a variation of Eq. 1, where q_t is replaced by q_e and C_t is replaced by C_e (mg L^{-1}; residual pharmaceutical concentration after shaking during the equilibrium time).

The obtained experimental data were fitted, using GraphPad Prism, version 5, to non-linear models commonly used to describe the adsorption equilibrium isotherms – Langmuir (Langmuir, 1918) and Freundlich (Freundlich, 1906) –, represented by Eq. (4) and (5), respectively:

$$q_e = \frac{q_m K_L C_e}{1 + K_L C_e} \quad \text{(Eq. 4)}$$

$$q_e = K_F C_e^{1/N} \quad \text{(Eq. 5)}$$

where q_m represents the maximum adsorption capacity (mg g^{-1}), C_e the amount of solute in the aqueous phase at equilibrium (mg L^{-1}), K_L (L mg^{-1}) the Langmuir affinity coefficient, N the degree of non-linearity, and K_F the Freundlich adsorption constant ($mg^{1-1/n}$ $L^{1/n}$ g^{-1}).

2.6 Micellar electrokinetic chromatography (MEKC) quantification

The quantification of CBZ, SMX and PAR in aqueous solutions during the adsorption experiments was performed by MEKC using a Beckman P/ACE MDQ instrument (Fullerton, CA, USA), equipped with a photodiode array detection system. A dynamically coated silica capillary with 40 cm (30 cm to the detection window) was used. The method used was adapted from Calisto et al. (2011). Briefly, the electrophoretic separation was accomplished at 25 ºC, in direct polarity mode at 25 kV, during 5 min runs and sample injection time of 4 s. Ethylvanillin was used as internal standard and sodium tetraborate was used to obtain better peak shape and resolution and higher repeatability, both spiked to all samples and standard solutions at final concentrations of 3.34 mg L^{-1} and 10 mM, respectively. Detection was monitored at 200 nm for SMX and PAR and at 214 nm for CBZ. Separation buffer consisted of 15 mM of sodium tetraborate and 30 mM of sodium dodecyl sulfate. Capillary was washed between each run with ultrapure water for 1 min and separation buffer for 1.5 min at 20 psi, at the beginning of each working day, with separation buffer for 20 min (to reload the dynamic coating), and at the end of the day, with ultrapure water for 10 min. All the analyses were performed in triplicate. For each pharmaceutical, calibration was

performed by analysing standard solutions with concentrations ranging from 0.25 and 5 mg L^{-1}. Standards were analysed in quadruplicate.

3. RESULTS AND DISCUSSION

3.1 Characterization of activated carbons

Regarding S_{BET} and microporosity, the AAC presented a S_{BET} of 1627 m^2 g^{-1} which was considered an excellent S_{BET} value comparing with the high-performance CAC used in the present study (S_{BET} 996 m^2 g^{-1}) and also comparing with other alternative adsorbents used in literature (alternative activated carbons with S_{BET} between 891 and 1060 m^2 g^{-1} (Mestre et al., 2007; Cabrita et al, 2010; Mestre et al., 2014)). The AAC presented also high prevalence of micropores (~68% of the total pore volume).

In what respects proximate and ultimate analysis, AAC presented high content in fixed carbon (~63%) and low content in ashes (~14%); CAC presented similar ashes content (~10%), but higher fixed carbon content (~86%). These results were consistent with the high TOC (67 ± 1%, for AAC and 80.9 ± 0.4, for CAC) and low IC (lower than 2% for both carbons) results. CAC presented a pH_{pzc} of ~7, while the pH_{pzc} of ~5 determined for AAC indicated that it presented an acidic surface, which was confirmed by the determination of the acidic oxygen-containing functional groups (carboxyl, lactones, and phenols) by the Boehm's titrations.

From the SEM images, it was observed that the AAC presented a high level of porosity, with an irregular surface and a well-defined presence of porous (which was in accordance with the N_2 adsorption isotherms) (Jaria et al., 2018); CAC presented some degree of porosity, but, for the same magnification, less roughness was observed in comparison with the AAC.

In what concerns XPS (Fig. 1), analysing the overall spectrum (Fig. 1a) it was possible to verify the high content in carbon (80.5%) and oxygen (18.5%) heteroatoms in the surface of AAC.

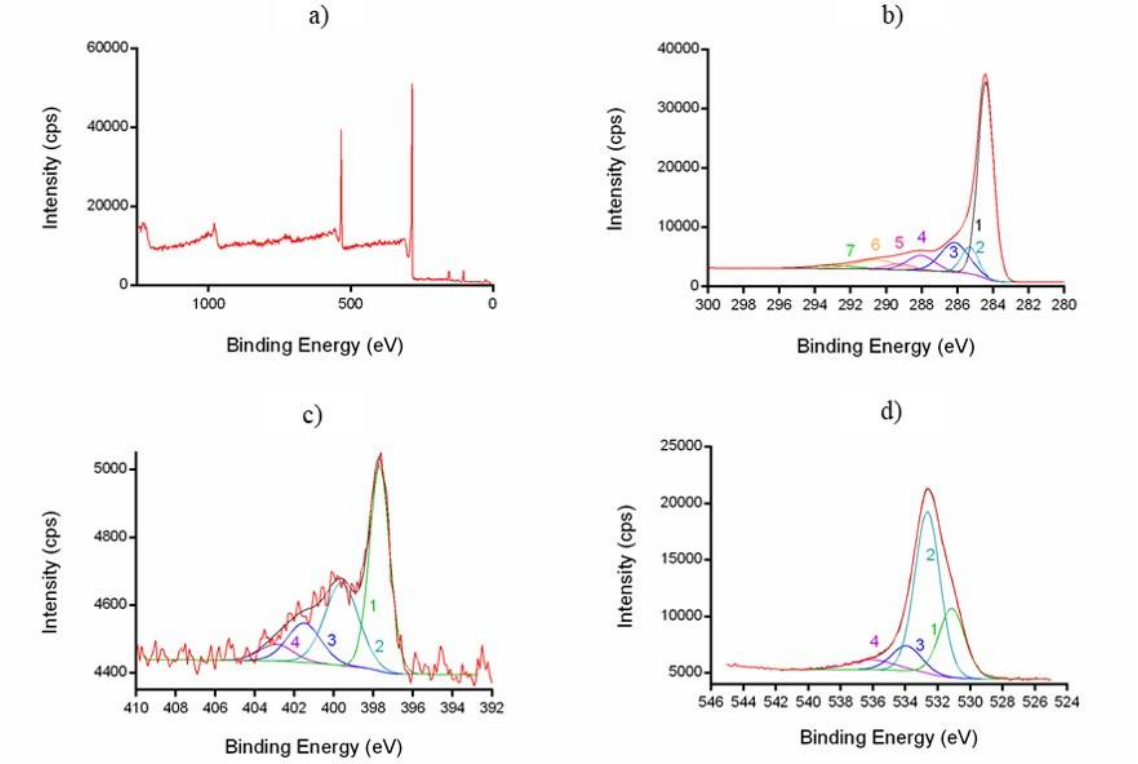

Fig. 1: XPS analysis for AAC: (a) AAC; (b) AAC-C1s; (c) AAC-N1s; (d) AAC-O1s.

By deconvolution of the C1s region (Fig. 1b) of the AAC spectrum, the presence of the graphitic Csp^2 (peak 1 – 284.4 eV which was the one presenting the highest intensity), the C–C sp^3 bond of the edge of the graphene layer (peak 2 – 285.3 eV), the C–O single bond, assigned to ether and alcohol groups (peak 3 – 286.1 eV), the O–C=O bond of carboxylic acids and/or carboxylic anhydride (peak 5 – 289.2 eV) and the π–π* transition in C1 (peak 6 – 290.5 eV), was evident. The N1s spectra (Fig. 1c) presented four main peaks: ~397.7 eV (peak 1), which may be attributed to pyridine nitrogen functional groups; ~399.6 eV (peak 2), that may be related to pyrrole or pyridine

functional groups; ~401.5 eV (peak 3), that may be assigned to quaternary nitrogen; and, finally, ~402.9 eV (peak 4) which may be attributed to the presence of oxidized forms of nitrogen (Fig. 1c). Concerning the O1s spectra (Fig. 1d), AAC presented a peak ~531.1 eV (peak 1) which may be assigned to the C=O group in quinones, and a peak ~532.6 (peak 2) which can be attributed to single bonded C–O–H (Abd-El-Aziz et al., 2008). There was also a peak at 533.9 eV (peak 3) that can be assigned to oxygen atoms in carboxyl groups (–COOH or COOR) and a peak ~536 eV (peak 4) that may be related to physisorbed water (Velo-Gala et al., 2014; Lee et al., 2016).

3.2 Biologically treated municipal wastewater

Results on the characterization of wastewater from the three collection campaings, namely pH, conductivity and TOC are depicted in Table 1.

Table 1: pH, conductivity and TOC values for the effluent samples.

Collection campaing	**1**	**2**	**3**
pH	7.7	7.8	7.9
Conductivity (mS cm^{-1})	8.5	9.2	5.8
TOC (mg L^{-1})	16.9	17.0	18.5

The analysed parameters showed that wastewater collected during the different campaings mantained similar properties. Therefore, the stability of the wastewater matrix for the adsorption experiments may be assumed.

3.3 Adsorption kinetics

The assessment of the time needed for the pharmaceuticals to achieve the equilibrium in the bulk solution/carbon surface interface is an important parameter

since, for the practical application of an adsorbent, it should not only present good adsorption capacities but also to adsorb in a suitable time scale. The results on the amount of each pharmaceutical adsorbed onto the AAC or the CAC at a time t (q_t, mg g^{-1}) *versus* time in ultrapure water and in wastewater are represented in Fig. 2 together with the corresponding fittings to pseudo-first and pseudo-second order kinetic models. The parameters obtained from the fittings of experimental results in ultrapure and wastewater are summarized in Table 2 and Table 3, respectively.

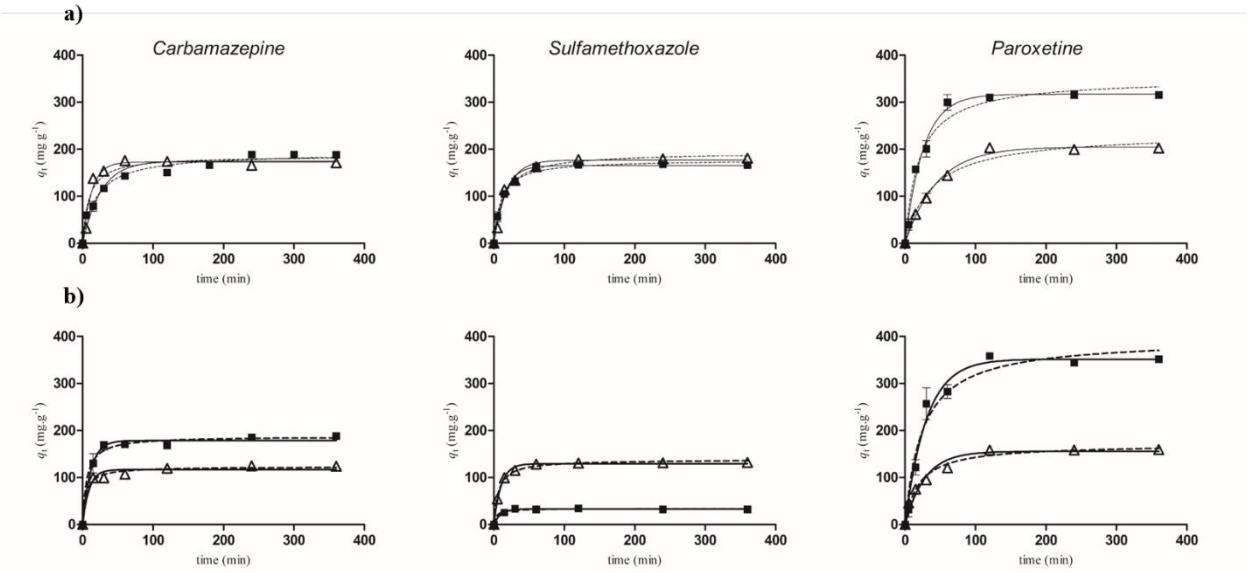

Fig. 2: Kinetic study of the adsorption of CBZ, SMX and PAR onto AAC (■) and CAC (∆) in (a) ultrapure water; (b) wastewater. Results were fitted to pseudo-first (full line) and pseudo-second (dashed line) order kinetic models. Each point (± standard deviation) is the average of three replicates. Experimental conditions: T = 25.0 ± 0.1 ºC; 80 rpm; $C_{i,\ pharmaceutical}$ = 5 mg L^{-1}; $C_{AAC\ or\ CAC}$ = 0.020 g L^{-1} (CBZ, SMX, PAR in ultrapure water); $C_{AAC\ or\ CAC}$ = 0.020 g L^{-1} (CBZ, PAR in wastewater); $C_{AAC\ or\ CAC}$ = 0.10 g L^{-1} (SMX in wastewater).

In ultrapure water, the kinetic experimental results onto AAC were better described by the pseudo-second than by pseudo-first order model with exception to PAR. Contrarily, the pseudo-first order model is the one that better described the pharmaceuticals' adsorption kinetics onto CAC. In any case, both models reasonably fitted experimental results ($R^2 \geq 0.93$). Comparing the adsorption of the selected

pharmaceuticals onto AAC and CAC, it can be verified that the CAC presented slighlty faster kinetics for CBZ but slower for SMX and PAR. However, the kinetic rate constants obtained for all systems were in the same order of magnitude and the equilibrium was quickly reached (60-240 min) onto both carbons, showing that they are kinetically adequate for the adsorption of the considered pharmaceuticals. In wastewater, except for PAR onto AAC, experimental results better fitted the pseudo-second than the pseudo-first order kinetic model. Still, both models may be considered adequate for the description of experimental results onto both AAC and CAC ($R^2 \geq$ 0.95). On the other hand, the time needed to attain the equilibrium in wastewater was not affected by matrix effects and the AAC continued to compare favourably with CAC. Still, in the case of SMX the adsorption was even faster in wastewater than in ultrapure water. Coimbra et al. (2015) had already observed that the matrix of an effluent from a STP, despite its complexity, did not affect the time needed to reach the equilibrium for pharmaceuticals (salicylic acid, diclofenac, ibuprofen, and acetaminophen), which was equally short in both ultrapure and wastewater.

3.4 Adsorption equilibrium

The adsorption isotherms, represented as the amount of each pharmaceutical adsorbed onto AAC and CAC at equilibrium (q_e, mg g^{-1}) *versus* the amount of pharmaceutical remaining in solution (C_e, mg L^{-1}), are shown in Fig. 3. Fitting parameters to Langmuir and Freundlich equilibrium models are summarized in Table 2 and Table 3, for isotherms determined in ultrapure and wastewater, respectively.

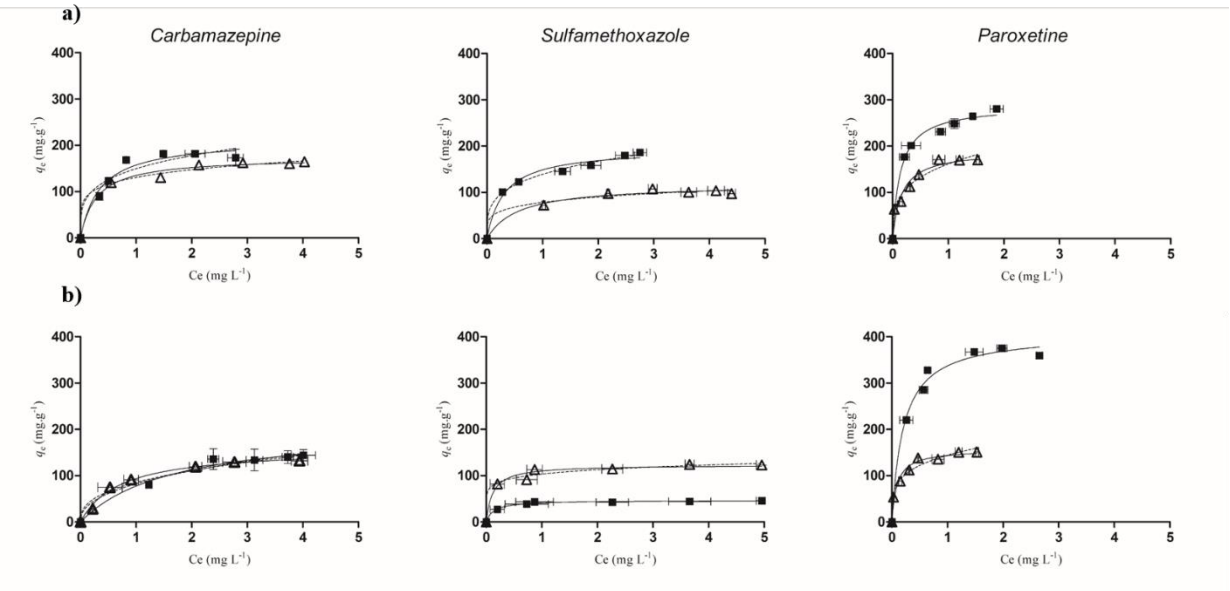

377

378 Fig. 3: Equilibrium study of the adsorption of CBZ, SMX and PAR onto AAC (■) and CAC (Δ)
379 in (a) ultrapure water; and (b) wastewater. Results were fitted to Langmuir (full line) and
380 Freundlich (dashed line) equilibrium models. Each point (± standard deviation) is the average of
381 three replicates. Experimental conditions: T = 25.0 ± 0.1 ºC; 80 rpm; $C_{i,\ pharmaceutical}$ = 5 mg L^{-1};
382 $C_{AAC\ or\ CAC}$ = 0.020 g L^{-1} (CBZ, SMX, PAR in ultrapure water); $C_{AAC\ or\ CAC}$ = 0.020 g L^{-1} (CBZ,
383 PAR in wastewater); $C_{AAC\ or\ CAC}$ = 0.10 g L^{-1} (SMX in wastewater).

384

385 In ultrapure water (Fig. 3a), experimental data were well described either by
386 Langmuir or Freundlich, with satisfactory correlation coefficients ($R^2 \geq 0.93$). As for the
387 Langmuir model, the AAC presented higher adsorption capacities (q_m between 194 and
388 287 mg g^{-1}) than CAC (q_m between 118 and 190 mg g^{-1}) for the three pharmaceuticals
389 tested. This difference may be related with the S_{BET} (1627 m^2 g^{-1} for AAC and 996 m^2 g^{-1} for CAC), which is one of the most important factors affecting the adsorption process.
391 Equilibrium isotherms in wastewater (Fig. 3b) also fitted both the Langmuir and
392 Freundlich models ($R^2 \geq 0.96$). Focusing on the Freundlich isotherm, it can be observed
393 that the adsorption isotherm was favourable ($N > 1$), for both carbons and matrices
394 (Tables 2 and 3), which points to the fact that the adsorbents are efficient removing both
395 high and low concentrations of the tested pharmaceuticals (Coimbra et al., 2015). In any

case, differences between equilibrium results in ultrapure water and wastewater were evident, which must be related to the fact of wastewater being a very complex matrix. For the adsorption of CBZ, either onto AAC or CAC, the type of matrix did not negatively affect the adsorption capacities, with q_m values in wastewater being similar to those obtained in ultrapure water. Also, in both matrices the adsorption capacity of CBZ onto AAC was higher than onto CAC. In the case of PAR, the adsorption capacity onto either AAC or CAC was higher in wastewater than in ultrapure water. This was especially evident for AAC (q_m 29% higher in wastewater than in ultrapure water), as for the comparison of the corresponding q_m in Tables 2 and 3. Also, the great difference between the adsorbent regarding the PAR adsorption capacity in wastewater has to be highlighted: the PAR q_m onto AAC was 62% higher than onto CAC. Finally, in the case of SMX, the adsorption capacity onto CAC remained the same in both matrices. However, in the case of SMX, the adsorption capacity onto AAC was larger than onto CAC in ultrapure water, but in wastewater the contrary was observed (lower capacity onto AAC than onto CAC). Furthermore, the q_m corresponding to SMX onto AAC was 76% lower in wastewater than in ultrapure water.

Adsorption, which is a rather complex process, is strongly ruled by electrostatic and non-electrostatic interactions. The influence of these interactions is directly governed by the characteristics of both the adsorbent (key parameters of the carbon's surface chemistry comprise its pH, surface functional groups and uptake of specific adsorbates per unit S_{BET} (Smith et al., 2009)) and the adsorbate (essential characteristics of the adsorbate are the octanol/water coefficient (log K_{ow}), the water solubility, the p*Ka* and the molecular size) (Calisto et al., 2015).

Table 2: Fitting parameters of pseudo-first and pseudo-second order kinetic models and of Langmuir and Freundlich equilibrium models to the experimental data for both carbons (AAC and CAC) and the three pharmaceuticals (CBZ, SMX, and PAR) in ultrapure water.

		CBZ		SMX		PAR	
		AAC	CAC	AAC	CAC	AAC	CAC
Pseudo	q_t (mg g^{-1})	175 ± 7	173 ± 6	165 ± 3	177 ± 5	317 ± 7	205 ± 5
1st order	k_1 (min^{-1})	0.038 ± 0.007	0.078 ± 0.013	0.066 ± 0.006	0.054 ± 0.006	0.039 ± 0.003	0.022 ± 0.002
	R^2	0.940	0.971	0.991	0.987	0.991	0.993
	S_{yx}	16.60	12.90	6.35	8.77	13.36	7.06
Pseudo	q_t (mg g^{-1})	192 ± 7	186 ± 12	178 ± 4	194 ± 7	351 ± 17	236 ± 13
2nd order	k_2 (mg g^{-1} min)	0.00027 ± 0.00005	0.00060 ± 0.00024	0.00056 ± 0.00007	0.00038 ± 0.00008	0.00014 ± 0.00003	0.00011 ± 0.00003
	R^2	0.974	0.934	0.993	0.982	0.976	0.979
	S_{yx}	10.81	19.34	5.54	10.04	21.76	12.63
Langmuir	q_m (mg g^{-1})	212 ± 16	174 ± 7	194 ± 10	118 ± 7	287 ± 9	190 ± 16
	K_l (L mg^{-1})	2.8 ± 0.8	3.5 ± 0.9	3.2 ± 0.7	1.8 ± 0.6	7 ± 1	6 ± 2
	R^2	0.965	0.986	0.979	0.982	0.991	0.941
	S_{yx}	13.73	7.58	10.05	5.58	9.94	16.17
Freundlich	K_f (mg g^{-1} (mg $L^{-1})^{-N}$)	149 ± 8	131 ± 4	139 ± 2	78 ± 6	Not	161 ± 5
	N	4 ± 1	5.80 ± 0.97	3.8 ± 0.2	5 ± 2	Converged	3.5 ± 0.4
	R^2	0.928	0.990	0.996	0.972		0.972
	S_{yx}	19.84	6.41	4.62	7.02		11.16

Table 3: Fitting parameters of pseudo-first and pseudo-second order kinetic models and of Langmuir and Freundlich equilibrium models to the experimental data for both carbons (AAC and CAC) and the three pharmaceuticals (CBZ, SMX, and PAR) in wastewater.

		CBZ		SMX		PAR	
		AAC	CAC	AAC	CAC	AAC	CAC
Pseudo	q_t (mg g^{-1})	179 ± 4	117 ± 4	32 ± 1	129 ± 2	352 ± 12	156 ± 7
1st order	k_1 (min^{-1})	0.09 ± 0.01	0.11 ± 0.03	0.32 ± 0.09	0.098 ± 0.007	0.033 ± 0.004	0.036 ± 0.006
	R^2	0.989	0.964	0.949	0.995	0.982	0.962
	S_{yx}	7.59	9.12	2.79	3.76	21.11	12.38
Pseudo	q_t (mg g^{-1})	188 ± 5	123 ± 4	33 ± 1	138 ± 2	396 ± 25	171 ± 6
2nd order	k_2 (mg g^{-1} min)	0.0009 ± 0.0002	0.0017 ± 0.0005	0.019 ± 0.007	0.0011 ± 0.0001	0.00010 ± 0.00003	0.00030 ± 0.00006
	R^2	0.990	0.986	0.969	0.995	0.966	0.984
	S_{yx}	7.22	5.61	2.17	3.66	29.10	8.12
Langmuir	q_m (mg g^{-1})	209 ± 27	160 ± 7	47 ± 1	123 ± 5	407 ± 14	156 ± 7
	K_l (L mg^{-1})	0.6 ± 0.2	1.4 ± 0.2	7.3 ± 1.2	8.4 ± 2.5	4.8 ± 0.8	11.0 ± 2.6
	R^2	0.984	0.991	0.992	0.975	0.99	0.975
	S_{yx}	8.12	5.32	1.60	7.61	14.92	9.14
Freundlich	K_f (mg g^{-1} (mg $L^{-1})^{-N}$)	82 ± 10	85 ± 6	Not	103 ± 3	Not	144 ± 4
	N	2.3 ± 0.5	2.65 ± 0.45	Converged	7.9 ± 1.5	Converged	4.2 ± 0.5
	R^2	0.975	0.956		0.981		0.975
	S_{yx}	10.03	11.88		6.66		9.26

The complexity involving the balance between these variables makes it very difficult to infer the effectiveness of adsorption in wastewater from results in ultrapure water. Therefore, although most of the studies on alternative adsorbents in literature do not contain such information, for the practical application of any adsorbent, experimentation in real matrices is essential.

In this work, it was found that each pharmaceutical behaved differently in wastewater as compared with ultrapure water. The adsorbents' and pharmaceuticals' charges at the wastewater pH may be underneath these differences. In general, an acidic surface favours the uptake of alkaline adsorbates and *vice versa*. In the case of AAC and CAC, the pH_{pzc} was around 5 and 7, respectively, which indicates that CAC is neutral while AAC presents an acidic surface. This was also observed by the determination of the acidic oxygen-containing functional groups by the Boehm's titrations: the surface chemistry of the AAC was mostly dominated by phenols and lactones (Jaria et al., 2018). Also, it is important to evaluate the main protonation state of the pharmaceuticals tested during the adsorption experiments. In wastewater (pH ~7.8), considering the p*Ka* values of the pharmaceuticals (pKa_{1CBZ} = 2.3, pKa_{2CBZ} = 13.9; pKa_{1SMX} = 5.7, pKa_{2SMX} = 1.8; pKa_{PAR} = 9.9) (Calisto et al., 2015), CBZ should be neutral, SMX negative and PAR positive. This may explain the marked decrease in the adsorption capacity of SMX onto AAC in wastewater.

It is well known that the SMX form depends greatly on the pH of the medium (Hou et al, 2013; Qi et al., 2014). Given the two p*Ka* values of SMX, for pH around 4, the non-protonated form is the predominant one, increasing pH to 7, most of the SMX molecules will be present in the deprotonated state and for a pH > 7, the predominant form of SMX will be the deprotonated one by the complete dissociation of the hydrogen present in the –NH– group (Qi et al., 2014). Therefore, SMX will be negatively charged

in wastewater (pH > 7) and will be mostly electrostatically repulsed by the also negatively charged AAC surface. Contrarily, CAC does not have a negatively charged surface, which may explain the non-decrease in the adsorption capacity of SMX. On the other hand, electrostatic interactions may be also responsible for the fact that in ultrapure water the differences between the adsorption capacities of AAC and CAC are not so accentuated. In ultrapure water pH is around 5.5-6 (much lower than that of wastewater) so changing the pharmaceuticals' speciation in comparison with wastewater.

Inversely to SMX, the adsorption of PAR onto AAC was favoured by the pH of the wastewater since PAR will be positively charged in that matrix. In the case of this pharmaceutical, the presence of one fluorine atom, which is the most electronegative halogen, may also count for strong hydrogen bonds with the AAC functional groups (this carbon presented carboxyl groups compatible with hydrogen bonding as it was defined in its characterization), increasing the affinity between adsorbate and adsorbent. Finally, as for CBZ, which is neutral at both the pH of ultrapure water and wastewater, no significant differences were observed between the q_m values of AAC in the two studied matrices.

The above results highlighted the importance of electrostatic interactions for the adsorption of pharmaceuticals and evidenced that the adsorption capacity of AAC, as that of any other adsorbent, is highly dependant on the protonation state of the target pharmaceutical, which, in turn, is governed by the aqueous matrix. It may therefore be advanced that the implementation of the optimized AAC, will be especially favourable for cations, followed by neutrals and lastly anions.

After having proved its good performance versus CAC, to further assess the efficiency of AAC in the removal of the selected pharmaceticals, a selection of the most relevant and recent literature (last ten years) on the utilization of alternative waste-based adsorbents for the removal of the considered pharmaceuticals was done. Table 4 summarizes the maximum adsorption capacity determined by different authors for these pharmaceuticals. Overall, most of the alternative adsorbents used for the target purpose originate from agrowastes and few from industrial wastes. Also, among the three pharmaceuticals here considered, SMX is the one that has received more attention in the literature, followed by CBZ and PAR. In any case, for the three pharmaceuticals, most of the studies have been carried out in ultrapure water. Very few works were carried out in real matrices or somehow evaluated matrix effects (e.g. Greiner et al., 2018; Naghdi et al., 2017; Shimabuku et al., 2014). Still, except for Oliveira et al. (2018), who used ACs from paper pulp and compared the adsorption of these pharmaceuticals from ultrapure and wastewater and Baghdadi et al. (2016), who used an optimally synthesized magnetic AC for the removal of CBZ, no results on the adsorption capacity of alternative adsorbents in wastewater were found. Safeguarding this important fact, data in Table 4 evidenced that, even in wastewater, the optimized AAC displayed a larger CBZ adsorption capacity than the other alternative adsorbents, except for the AC produced from pomelo peel by Chen et al. (2017) under a two-step pyrolysis procedure. The latter is the waste-based adsorbent that, to the best of our knowledge, possesses the largest CBZ adsorption capacity in ultrapure water, this value being only slightly higher than q_m values here determined for AAC in wastewater. With respect to SMX, the adsorption capacity of AAC here determined in ultrapure water is quite relevant as compared with results in the literature (Table 4). On the other hand, the adsorption capacity of AAC in wastewater is higher than most of the values determined for other

501 Table 4: Adsorption capacity of alternative waste-based adsorbents reported in literature for the removal of CBZ, PAR or SMX.

Pharmaceutical	Waste-based adsorbent	Matrix	Isotherm Conditions[a]	Adsorption capacity[b] (mg g^{-1})	Reference
CBZ	AC from coconut shell	Ultrapure water	T = 23ºC	*57.6*	Yu et al., 2008
	Rice straw	Ultrapure water	T = 28 ºC; pH = 6.5	*28.6*	Liu et al., 2013
	Biochar from paper mill sludge	Ultrapure water	T = 25 ºC; pH = 10.5	*12.6*	Calisto et al., 2015
	Magnetic AC from coconut, pinenut and walnut shells	Ultrapure water	T = 25 ºC; pH = 6	*135.1*	Shan et al., 2016
	Magnetic nanocomposite of AC	Biologically treated sewage	T = 25 ºC; pH = 6.65	*182.9*	Baghdadi et al., 2016
	AC from pomelo peel	Ultrapure water	T = 25 ºC; pH = 4.4	*286.5*	Chen et al., 2017
	Pine-wood derived nanobiochar		T = 25 ºC; pH = 6	*40*	Naghdi et al., 2017
	AC from palm kernel shell	Ultrapure water	T = 25 ºC; pH = 7	*189*	To et al., 2017
	AC from bleached paper pulp	Ultrapure water	T = 25 ºC	*93*	Oliveira et al., 2018
		Biologically treated sewage	T = 25 ºC; pH = 7.8	*80*	
	Optimized AC from paper mill sludge	Ultrapure water	T = 25 ºC	*212*	This study
		Biologically treated sewage	T = 25 ºC; pH = 7.8	*209*	
PAR	Biochar from paper mill sludge	Ultrapure water	T = 25 ºC; pH = 10.5	*38*	Calisto et al., 2015
	Optimized AC from paper mill sludge	Ultrapure water	T = 25 ºC	*287*	This study
		Biologically treated sewage	T = 25 ºC; pH = 7.8	*407*	
SMX	Walnut shells	Ultrapure water	T = 20 ºC; pH = 7	*0.47*	Teixeira et al., 2012
	Rice straw biochar	Ultrapure water	T = 25 ºC; pH = 3	*1.8*	Han et al., 2013
	Biochar from paper mill sludge	Ultrapure water	T = 25 ºC; pH = 10.5	*1.69*	Calisto et al., 2015
	Rice straw biochar	Ultrapure water	T = 25 ºC; pH = 6	*4.2*	Sun et al., 2016
	Spent mushroom substrate	Ultrapure water	T = 15 ºC; pH = 3	*2.4*	Zhou et al., 2016
	Functionalized bamboo biochar	Ultrapure water	T = 25 ºC; pH = 3.25	*88.10*	Ahmed et al., 2017
	Hybrid clay nanosorbent	Ultrapure water	T = 25 ºC; pH = 7	*152*	Martínez-Costa et al., 2018
	AC from bleached paper pulp	Ultrapure water	T = 25 ºC	*110*	Oliveira et al., 2018
		Biologically treated sewage	T = 25 ºC; pH = 7.8	*13.3*	
	Biochar from anaerobically digested bagasse	Ultrapure water	T = 25 ºC; pH = 6.5	*23.2*	Reguyal and Sarmah, 2018
	Modified organic vermiculites	Ultrapure water	T = 22 ºC; pH ≈ 6	*54.4*	Yao et al., 2018
	AC from almond shell	Ultrapure water	---	*344.8*	Zbair et al., 2018

AC from walnut shells	Ultrapure water	T = 30 ºC; pH = 5.5 (optimized conditions)	*106.9*	Teixeira et al., 2019
Optimized AC from paper mill sludge	Ultrapure water	T = 25 ºC	*194*	This study
	Biologically treated sewage	T = 25 ºC; pH = 7.8	*47*	
	Biologically treated sewage	T = 25 ºC; pH = 7.8	*407*	

[a]The temperature (T) at which isotherms were experimentally determined under batch stirred operation together with the pH of the aqueous matrix (if available); [b]Maximum capacity values resulting from model fittings of the experimental isotherms.

504 materials in ultrapure water and higher than the capacity of the AC from bleached paper
505 pulp in wastewater (Oliveira et al., 2018). It must be pointed out that the largest SMX
506 capacity in ultrapure water reported in the literature for an alternative adsorbent was
507 determined by Zbair et al. (2018) for an AC produced from almond shell in a two-step
508 pyrolysis and using hydrogen peroxide as activating agent in a ratio 1:10 (carbon from
509 the first pyrolysis/hydrogen peroxide). This AC was used in adsorption experiments
510 carried out under stirring in an ultrasonic bath, with no specification of the temperature
511 at which the isotherms were determined. Finally, regarding PAR, scarce results on the
512 adsorption capacity of waste-based adsorbents were found in the literature. In any case,
513 Table 4 evidences that the optimized AAC in this work displayed very remarkable
514 capacities in ultrapure and, especially, in wastewater.

515

516 **4. CONCLUSIONS**

517 The AAC produced from paper mill sludge under an optimized procedure
518 displayed fast adsorption kinetics for the three pharmaceuticals considered (CBZ, PAR
519 and SMX), being as good as the high-performance CAC used for comparison. Kinetics
520 were equally fast in ultrapure and in biologically treated wastewater. The equilibrium
521 isotherms evidenced the better performance of AAC than CAC in ultrapure water;
522 however, in wastewater, equilibrium results onto AAC were affected by matrix effects
523 depending on the pharmaceutical. Thus, comparing ultrapure water and wastewater, q_m
524 of CBZ remained similar , was larger for PAR and lower for SMX. Matrix effects were
525 not so evident in the case of adsorption onto CAC, which was related to differences in
526 the surface charge of the carbons (neutral in the case of CAC and acidic in the case of
527 AAC). Overall, it was demonstrated that the optimized paper mill sludge-based AC is a
528 very good adsorbent for pharmaceuticals in water with high potential to be applied at a

tertiary stage in wastewater treatment. Still, it was proved the necessity of carrying out adsorption studies in wastewater, in view of the practical application in real systems. Also, future developments of this work should include the evaluation of the adsorptive performance under competitive conditions considering a mixture of pharmaceuticals. These latter conclusions are probably applicable to any adsorbent to be used for the removal of pharmaceuticals and contrast with the fact that most of the published results are obtained in ultrapure (or distilled) water and in single component systems.

ACKNOWLEDGMENTS

This work was funded by FEDER through COMPETE 2020 and by national funds through FCT by the research project PTDC/AAG-TEC/1762/2014. Vânia Calisto and Marta Otero also thank FCT for a postdoctoral grant (SFRH/BPD/78645/2011) and support by the FCT Investigator Program (IF/00314/2015), respectively. Thanks are also due for the financial support to CESAM (UID/AMB/50017-POCI-01-0145-FEDER-007638), to FCT/MCTES through national funds (PIDDAC), and the co-funding by the FEDER, within the PT2020 Partnership Agreement and Compete 2020. M. Fontes and workers of Aveiro's STP (Águas do Centro Litoral) are gratefully acknowledged for assistance on the effluent samplings.

REFERENCES

Abd-El-Aziz As, Carraher CE, Pittman CU, Zeldin M. 2008. Inorganic and Organometallic Macromolecules: Design and Applications. Springer-Verlag New York.

AENOR. 1984. Solid mineral fuels. Determination of ash. Asociación Española de Normalización y Certificación.

AENOR. 1985. Hard coal and coke. Determination of volatile matter content. Asociación Española de Normalización y Certificación.

AENOR. 1995. Solid mineral fuels. Determination of moisture in the analysis sample. Asociación Española de Normalización y Certificación.

Ahmed MB, Zhou JL, Ngo HH, Guo W, Johir MAH, Sornalingam K. 2017. Single and competitive sorption properties and mechanism of functionalized biochar for removing sulfonamide antibiotics from water. *Chem. Eng. J.* 311:348–358.

Baghdadi M, Ghaffari E, Aminzadeh B. 2016. Removal of carbamazepine from

561 municipal wastewater effluent using optimally synthesized magnetic activated
562 carbon: Adsorption and sedimentation kinetic studies. *J. Environ. Chem. Eng.* 4:
563 3309–3321.
564 Brunauer S, Emmett PH, Teller E. 1938. Adsorption of gases in multimolecular layers.
565 *J. Am. Chem. Soc.* 60:309–319.
566 Cabrita I, Ruiz B, Mestre AS, Fonseca IM, Carvalho AP, Ania CO. 2010. Removal of
567 an analgesic using activated carbons prepared from urban and industrial residues.
568 *Chem. Eng. J.* 163:249–255.
569 Calisto V, Domingues MRM, Erny GL, Esteves VI. 2011. Direct photodegradation of
570 carbamazepine followed by micellar electrokinetic chromatography and mass
571 spectrometry. *Water Res.* 45:1095–1104.
572 Calisto V, Ferreira CIA, Santos SM, Gil MV, Otero M, Esteves VI. 2014. Production of
573 adsorbents by pyrolysis of paper mill sludge and application on the removal of
574 citalopram from water. *Biores. Technol.* 166:335–344.
575 Calisto V, Ferreira CIA, Oliveira JABP, Otero M, Esteves VI. 2015. Adsorptive
576 removal of pharmaceuticals from water by commercial and waste-based carbons. *J.*
577 *Environ. Manage.* 152:83–90.
578 Chen D, Xie S, Chen C, Quan H, Hua L, Luo X, Guoa L. 2017. Activated biochar
579 derived from pomelo peel as a high-capacity sorbent for removal of carbamazepine
580 from aqueous solution. *RSC Advances* 7:54969–54979.
581 Coimbra RN, Calisto V, Ferreira CIA, Esteves VI, Otero M. 2015. Removal of
582 pharmaceuticals from municipal wastewater by adsorption onto pyrolyzed pulp
583 mill sludge. *Arab. J. Chem. in press*. DOI: 10.1016/j.arabjc.2015.12.001.
584 Dubinin MM. 1966. Properties of active carbons, In: Chemistry and Physics of Carbon.
585 Marcel Dekker Inc., New York, pp. 51–120.
586 Freundlich H. 1906. Über die Adsorption in Lösungen. Z. für. *Phys. Chem.* 57:385–447.
587 Grace MA, Clifford E, Healy MG. 2016. The potential for the use of waste products
588 from a variety of sectors in water treatment processes. *J. Clean. Prod.* 137:788–
589 802.
590 Greiner B.G., Shimabuku, K.K., Summers, R.S. 2018. Influence of biochar thermal
591 regeneration on sulfamethoxazole and dissolved organic matter adsorption. *Env.*
592 *Sci.: Water Res. Tech.* 4: 169–174.
593 Han X, Liang C, Li T, Wang K, Huang H, Yang X. 2013. Simultaneous removal of
594 cadmium and sulfamethoxazole from aqueous solution by rice straw biochar. *J.*
595 *Zhejiang Univ. Sci. B* 14:640–649.
596 Ho IS, McKay G. 1999. Pseudo-second order model for sorption processes. *Process*
597 *Biochem.* 34:451–465.
598 Hou L, Zhang H, Wang L, Chen L, Xiong Y, Xue X. 2013. Removal of
599 sulfamethoxazole from aqueous solution by sono-ozonation in the presence of a
600 magnetic catalyst. *Sep. Purif. Technol.* 117:46–52.
601 Jaria G, Calisto V, Gil MV, Otero M, Esteves VI. 2015. Removal of fluoxetine from
602 water by adsorbent materials produced from paper mill sludge. *J. Colloid Interface*
603 *Sci.* 448:32–40.
604 Jaria G, Silva CP, Oliveira JABP, Santos SM, Gil MV, Otero M, Calisto V, Esteves VI.

605 2018. Production of highly efficient activated carbons from industrial wastes for
606 the removal of pharmaceuticals from water – a full factorial design. *J. Hazard*
607 *Mater. in press* DOI: 10.1016/j.jhazmat.2018.02.053.
608 Lagergren SY. 1898. Zur Theorie der sogenannten Adsorption geloster Stoffe. *K. Sven.*
609 *Vetenskapsakademiens* 24:1–3.
610 Langmuir I. 1918. The Adsorption of Gases on Plane Surfaces of Glass, Mica and
611 Platinum. *J. Am. Chem. Soc.* 40:1361–1403.
612 Lee MS, Park M, Kim HY, Park SJ. 2016. Effects of Microporosity and Surface
613 Chemistry on Separation Performances of N-Containing Pitch-Based Activated
614 Carbons for CO2/N2 Binary Mixture. *Sci. Rep.* 6:23224.
615 Liu Z, Zhou X, Chen X, Dai C, Zhang J, Zhang Y. 2013. Biosorption of clofibric acid
616 and carbamazepine in aqueous solution by agricultural waste rice straw. *J. Environ.*
617 *Sci.* 25:2384–2395.
618 Martínez-Costa JI, Leyva-Ramos R, Padilla-Ortega E, Aragón-Piña A, Carrales-
619 Alvarado DH. 2018. Antagonistic, synergistic and non-interactive competitive
620 sorption of sulfamethoxazole-trimethoprim and sulfamethoxazole-cadmium (ii) on
621 a hybrid clay nanosorbent. *Sci. Total Environ.* 640-641:1241–1250.
622 Mestre AS, Pires J, Nogueira JMF, Carvalho AP. 2007. Activated carbons for the
623 adsorption of ibuprofen. *Carbon* 45:1979–1988.
624 Mestre AS, Pires J, Nogueira JMF, Parra JB, Carvalho AP, Ania CO. 2009. Waste-
625 derived activated carbons for removal of ibuprofen from solution: Role of surface
626 chemistry and pore structure. *Bioresour. Technol.* 100:1720–1726.
627 Mestre AS, Bexiga AS, Proença M, Andrade M, Pinto ML, Matos I, Fonseca IM,
628 Carvalho AP. 2011. Activated carbons from sisal waste by chemical activation with
629 K_2CO_3: Kinetics of paracetamol and ibuprofen removal from aqueous solution.
630 *Bioresour. Technol.* 102:8253–8260.
631 Mestre AS, Pires RA, Aroso I, Fernandes EM, Pinto ML, Reis RL, Andrade MA, Pires
632 J, Silva SP, Carvalho AP. 2014. Activated carbons prepared from industrial pre-
633 treated cork: Sustainable adsorbents for pharmaceutical compounds removal.
634 *Chem. Eng.* J. 253:408–417.
635 Naghdi, M., Taheran, M., Pulicharla, R., Rouissi, T., Brar, S.K., Verma, M., Surampalli,
636 R.Y. 2017. Pine-wood derived nanobiochar for removal of carbamazepine from
637 aqueous media: Adsorption behavior and influential parameters. *Arab. J. Chem.*
638 DOI: 10.1016/j.arabjc.2016.12.025.
639 Oliveira G, Calisto V, Santos SM, Otero M, Esteves VI. 2018. Paper pulp-based
640 adsorbents for the removal of pharmaceuticals from wastewater: A novel approach
641 towards diversification. *Sci. Total Environ.* 631-632:1018–1028.
642 Qi C, Liu X, Lin C, Zhang X, Ma J, Tan H, Ye W. 2014. Degradation of
643 sulfamethoxazole by microwave-activated persulfate: Kinetics, mechanism and
644 acute toxicity. *Chem. Eng. J.* 249:6–14.
645 Reguyal F, Sarmah AK. 2018. Adsorption of sulfamethoxazole by magnetic biochar:
646 Effects of pH, ionic strength, natural organic matter and 17α-ethinylestradiol. *Sci.*
647 *Total Environ.* 628-629:722–730.
648 Silva CP, Jaria G, Otero M, Esteves VI, Calisto V. 2017. Waste-based alternative

adsorbents for the remediation of pharmaceutical contaminated waters: Has a step forward already been taken? *Bioresour. Technol.* 250:888–901.

Shan D, Deng S, Zhao T, Wang B, Wang Y, Huang J, Yu G, Winglee J, Wiesner MR. 2016. Preparation of ultrafine magnetic biochar and activated carbon for pharmaceutical adsorption and subsequent degradation by ball milling. *J. Hazard. Mater.* 305:156–163.

Shimabuku KK, Cho H, Townsend EB, Rosario-Ortiz FL, Summers, RS. 2014. Modeling nonequilibrium adsorption of MIB and sulfamethoxazole by powdered activated carbon and the role of dissolved organic matter competition. *Env. Sci. Tech.* 48:13735–13742.

Smith KM, Fowler GD, Pullket S, Graham NJD. 2009. Sewage sludge-based adsorbents: A review of their production, properties and use in water treatment applications. *Water Res.* 43:2569–2594.

Sun B, Lian F, Bao Q, Liu Z, Song Z, Zhu L. 2016. Impact of low molecular weight organic acids (LMWOAs) on biochar micropores and sorption properties for sulfamethoxazole. *Environ. Pollut.* 214:142–148.

Teixeira S, Delerue-Matos C, Santos L. 2012. Removal of sulfamethoxazole from solution by raw and chemically treated walnut shells. *Environ. Sci. Pollut. Res.* 19:3096–3106.

Teixeira S, Delerue-Matos C, Santos L. 2019. Application of experimental design methodology to optimize antibiotics removal by walnut shell based activated carbon. *Sci. Total Environ.* 646:168–176.

To M-H, Hadi P, Hui C-W, Lin CSK, McKay G. 2017. Mechanistic study of atenolol, acebutolol and carbamazepine adsorption on waste biomass derived activated carbon. *J. Mol. Liq.* 241:386–398.

Velo-Gala I, López-Peñalver JJ, Sánchez-Polo M, Rivera-Utrilla J. 2014. Surface modifications of activated carbon by gamma irradiation. *Carbon* 67:236–249.

Yao Y, Zhang Y, Gao B, Chen R, Wu F. 2018. Removal of sulfamethoxazole (SMX) and sulfapyridine (SPY) from aqueous solutions by biochars derived from anaerobically digested bagasse. *Environ. Sci. Poll. Res.* 25(26):25659–25667.

Yu Z, Peldszus, S, Huck, PM. 2008. Adsorption characteristics of selected pharmaceuticals and an endocrine disrupting compound-Naproxen, carbamazepine and nonylphenol-on activated carbon. *Water Res.* 42:2873–2882.

Zbair M, Ait Ahsaine H, Anfar Z. 2018. Porous carbon by microwave assisted pyrolysis: An effective and low-cost adsorbent for sulfamethoxazole adsorption and optimization using response surface methodology. *J. Clean. Prod.* 202:571–581.

Zhou A, Zhang Y, Li R, Su X, Zhang L. 2016. Adsorptive removal of sulfa antibiotics from water using spent mushroom substrate, an agricultural waste. *Desalin. Water Treat.* 57:388–397.

FIGURE CAPTIONS

Fig. 1: XPS analysis for AAC: (a) AAC; (b) AAC-C1s; (c) AAC-N1s; (d) AAC-O1s.

Fig. 2: Kinetic study of the adsorption of CBZ, SMX and PAR onto AAC (■) and CAC (Δ) in (a) ultrapure water; (b) wastewater. Results were fitted to pseudo-first (full line) and pseudo-second (dashed line) order kinetic models. Each point (± standard deviation) is the average of three replicates. Experimental conditions: T = 25.0 ± 0.1 ºC; 80 rpm; $C_{i,\ pharmaceutical}$ = 5 mg L^{-1}; $C_{AAC\ or\ CAC}$ = 0.020 g L^{-1} (CBZ, SMX, PAR in ultrapure water); $C_{AAC\ or\ CAC}$ = 0.020 g L^{-1} (CBZ, PAR in wastewater); $C_{AAC\ or\ CAC}$ = 0.10 g L^{-1} (SMX in wastewater).

Fig. 3: Equilibrium study of the adsorption of CBZ, SMX and PAR onto AAC (■) and CAC (Δ) in (a) ultrapure water; and (b) wastewater. Results were fitted to Langmuir (full line) and Freundlich (dashed line) equilibrium models. Each point (± standard deviation) is the average of three replicates. Experimental conditions: T = 25.0 ± 0.1 ºC; 80 rpm; $C_{i,\ pharmaceutical}$ = 5 mg L^{-1}; $C_{AAC\ or\ CAC}$ = 0.020 g L^{-1} (CBZ, SMX, PAR in ultrapure water); $C_{AAC\ or\ CAC}$ = 0.020 g L^{-1} (CBZ, PAR in wastewater); $C_{AAC\ or\ CAC}$ = 0.10 g L^{-1} (SMX in wastewater).